Electronic Supplementary Material (ESI) for Physical Chemistry Chemical Physics.

Supporting Information: Synthesis and composition modification of precipitate tubes in a confined flow reactor

Kinga Bene, Edina Balog, and Gábor Schuszter*

Department of Physical Chemistry and Materials Science, University of Szeged, Rerrich Béla tér 1., Szeged, H-6720, Hungary

E-mail: schuszti@chem.u-szeged.hu

Contents

S1 Macroscopic alkaline earth metal–carbonate precipitate patterns

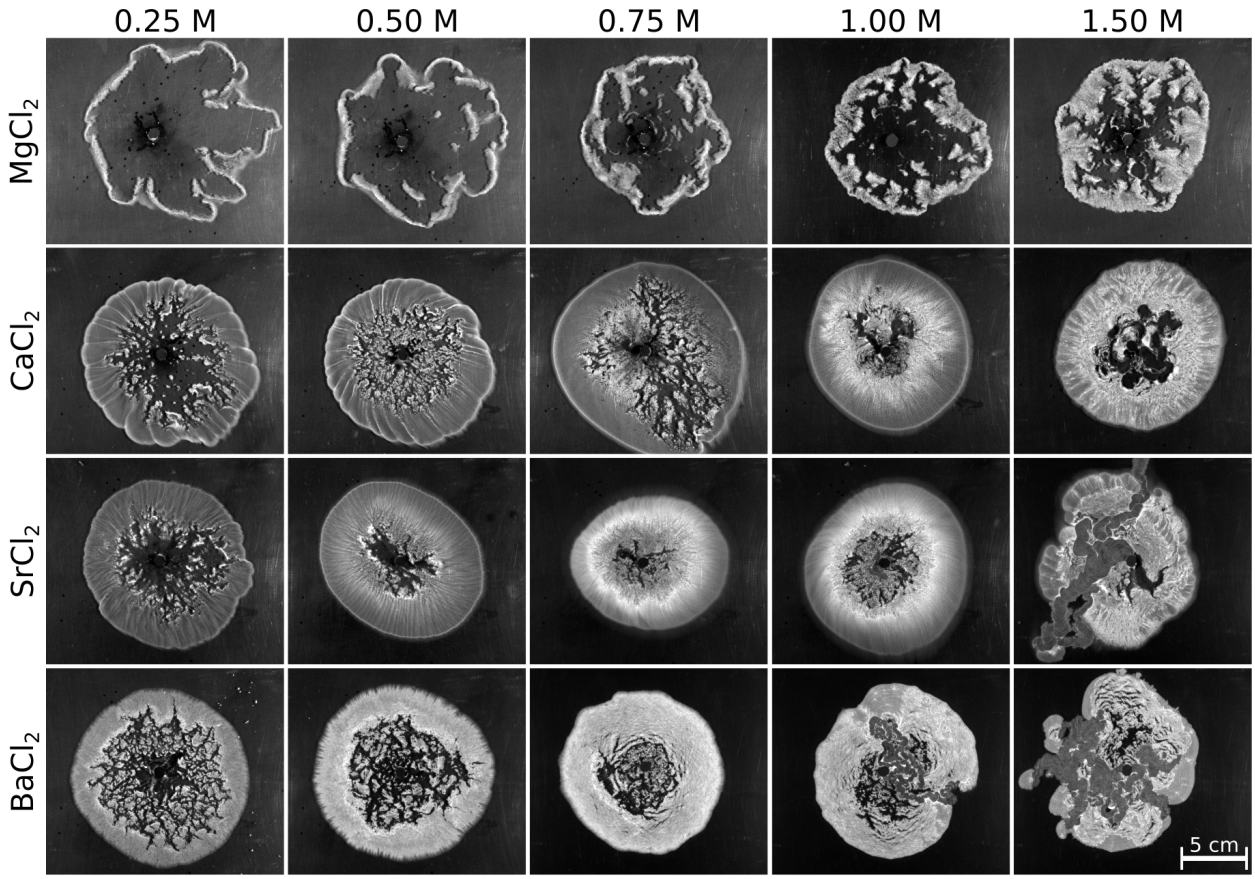

Figure S1: Macroscopic patterns of alkaline earth metal–carbonate precipitation systems at different alkaline earth metal concentrations. $c_{Na_2CO_3} = 1.5\,\mathrm{M}$; $Q = 1\,\mathrm{mL/min}$; $V_{Na_2CO_3} = 5\,\mathrm{mL}$.

S2 Quantitative analysis of calcium containing macroscopic precipitate patterns

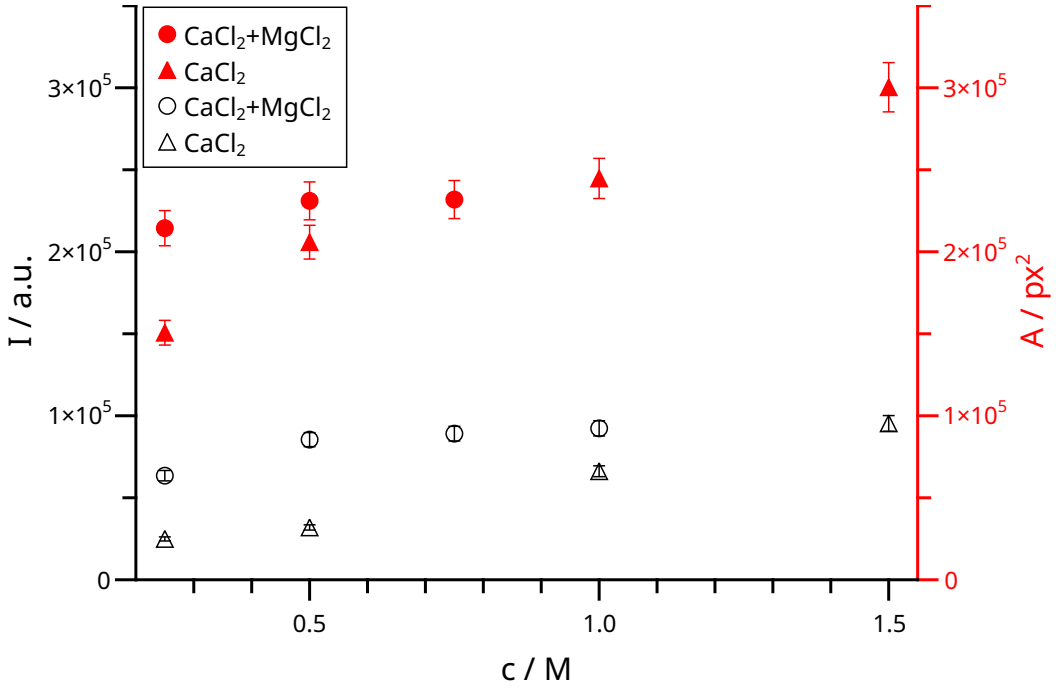

Figure S2: Dependence of picture grayscale intensity (I, empty symbols) and precipitate covered area (A, filled symbols) as a function of calcium chloride concentration in case of calcium–carbonate and calcium–magnesiu–carbonate precipitation systems. $c_{Na_2CO_3} = 1.5\,M$; $c_{MgCl_2} = 1.5\,M$; $Q = 1\,mL/min$; $V_{Na_2CO_3} = 5\,mL$.

S3 Optical microscopic analysis of membrane segment of the patterns

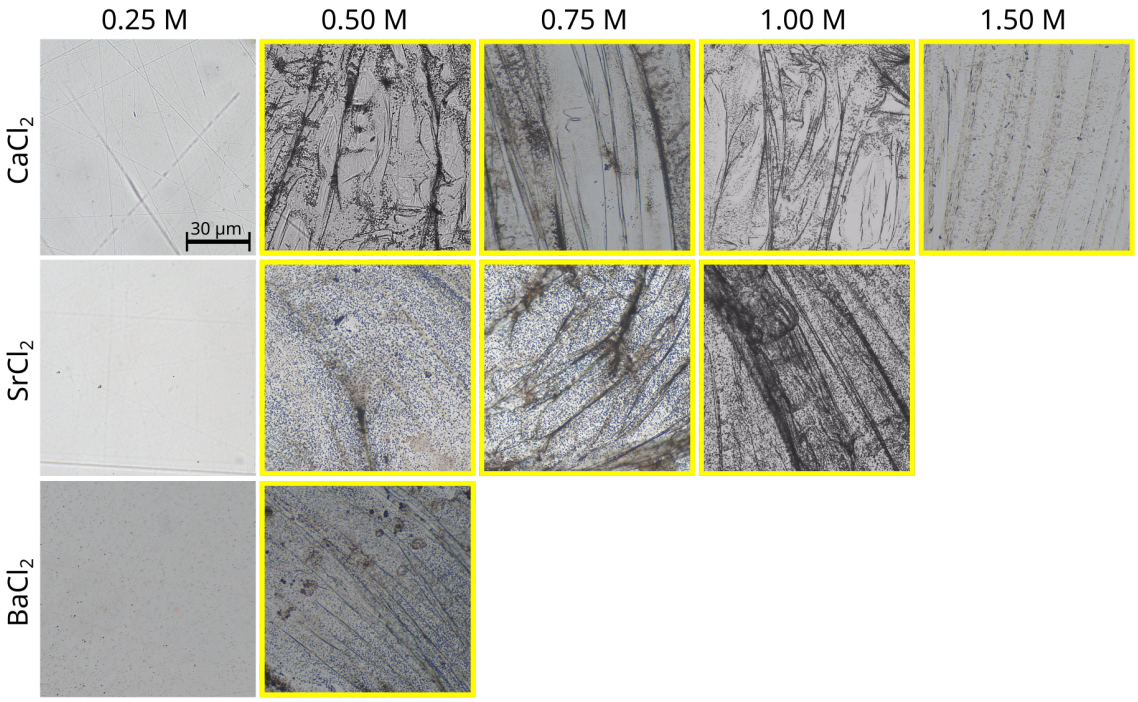

Figure S3: Optical microscope images of the composite alkaline earth metal–carbonate precipitate patterns at different added alkaline earth metal ion concentration. The microscope images, where the precipitate membrane structure is observed on macro scale, are marked with yellow frame. $c_{Na_2CO_3} = 1.5\,M$; $c_{MgCl_2} = 1.5\,M$; $Q = 1\,mL/min$; $V_{Na_2CO_3} = 5\,mL$.

S4 Powder X-ray diffractograms of pure and composite strontium and calcium containing precipitates

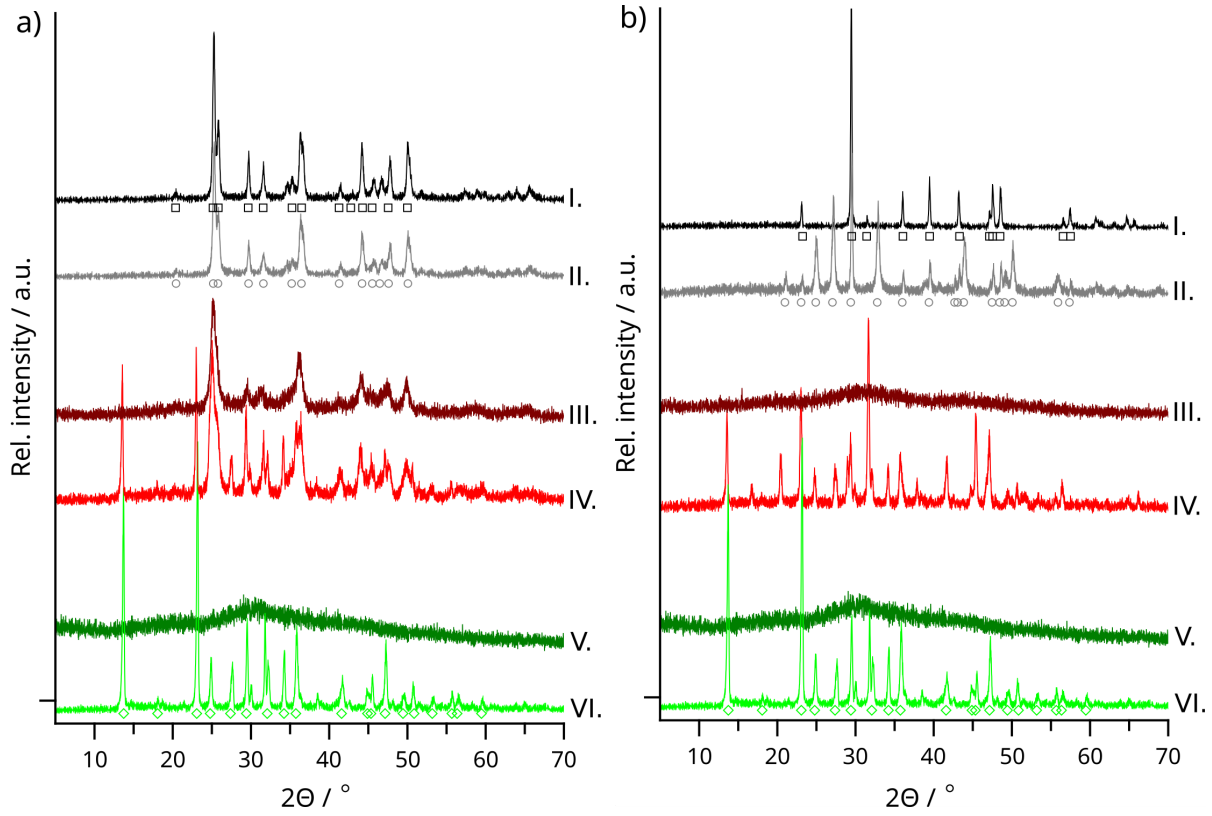

Figure S4: Powder X-ray diffractograms of **a**: pure strontium–carbonate system in flow-driven (**I.**) and well-stirred (**II.**) medium, composite strontium–magnesium–carbonate system in flow-driven (**III.**) and well-stirred (**IV.**) medium, magnesium-containing precipitate in flow-driven (**V.**) and well-stirred (**VI.**) medium; **b**: pure calcium–carbonate system in flow-driven (calcite) (**I.**) and well-stirred (vaterite) (**II.**) medium, composite calcium–magnesium–carbonate system in flow-driven (**III.**) and well-stirred (**IV.**) medium, magnesium-containing precipitate in flow-driven (**V.**) and well-stirred (**VI.**) medium. Symbols below the diffractograms correspond to published diffractions of various precipitates;[1–4] see Table S2 and S3 for more information. $c_{Na_2CO_3} = c_{MgCl_2} = 1.5\,M$; $c_{CaCl_2,SrCl_2} = 0.5\,M$; $Q = 1\,mL/min$; $V_{Na_2CO_3} = 5\,mL$.

Table S1: The exact position ($2\Theta\,/\,^\circ$) of the assigned diffractions of the PXRD patterns presented in Fig. 5b in the manuscript, and the corresponding Miller indices (hkl; obtained from Match! database). Materials I and II are identical ($BaCO_3$), materials III and IV are also identical (norsethite, $BaMg(CO_3)_2$), material V is amorphous, while material VI is nesquehonite, $MgCO_3.3H_2O$.

$2\Theta/^\circ$ (I and II)	$BaCO_3$ (hkl)	$2\Theta/^\circ$ (III and IV)	norsethite (hkl)	$2\Theta/^\circ$ (VI)	nesquehonite (hkl)
19.495	(110)	15.881	(003)	13.558	$(10\bar{1})$
19.946	(020)	21.159	(101)	18.061	(011)
23.962	(111)	23.094	(102)	23.068	(200)
24.315	(021)	29.661	(104)	24.782	$(\bar{1}03)$
27.803	(002)	31.995	(006)	27.380	$(20\bar{2})$
34.185	(112)	33.819	(105)	29.405	$(21\bar{1})$
34.615	(130)	35.858	(110)	32.077	$(21\bar{2})$
39.584	(220)	39.439	(113)	34.193	(021)
42.112	(221)	42.008	(201)	35.739	$(30\bar{1})$
45.036	(132)	43.083	(202)	41.582	$(30\bar{3})$
47.158	(023)	47.200	(204)	44.380	(006)
		48.286	(108)	45.337	(313)
		48.837	(116)	47.143	(223)
		57.195	(212)	49.434	$(\bar{3}14)$
		60.665	(214)	50.707	(025)
		63.144	(215)	53.173	(131)
		64.443	(300)	55.676	(413)
				56.349	$(\bar{2}25)$
				59.462	$(42\bar{1})$

Table S2: The exact position ($2\Theta\,/^\circ$) of the assigned diffractions of the PXRD patterns presented in Fig. S4a, and the corresponding Miller indices (hkl; obtained from Match! database). Materials I and II are identical ($SrCO_3$), material III depicts most diffractions of $SrCO_3$, material IV depicts diffractions corresponding to both $SrCO_3$ and nesquehonite ($MgCO_3.3H_2O$), material V is amorphous, while material VI is nesquehonite. Color coding used in the last column helps the assignment of the material.

$2\Theta/^\circ$ (I. and II.)	$2\Theta/^\circ$ (III.)	$2\Theta/^\circ$ (IV.)	$2\Theta/^\circ$ (VI.)	$SrCO_3$, nesquehonite (hkl)
		13.558	13.558	$(10\bar{1})$
		18.061	18.061	(011)
20.375				(110)
		23.068	23.068	(200)
			24.782	$(\bar{1}03)$
25.230	25.230	25.230		(111)
25.806	25.806	25.806		(021)
		27.380	27.380	$(20\bar{2})$
		29.405	29.405	$(21\bar{1})$
29.696	29.696			(002)
31.590	31.590			(012)
		32.077	32.077	$(21\bar{2})$
		34.193	34.193	(021)
34.619				(102)
35.202				(200)
			35.739	$(30\bar{1})$
36.521	36.521	36.521		(130)
41.325	41.325			(220)
		41.582	41.582	$(30\bar{3})$
44.200	44.200	44.200		(221)
			44.380	(006)
			45.337	(313)
45.644	45.644	45.644		(041)
46.702				(202)
			47.143	(223)
47.705	47.705	47.705		(132)
			49.434	$(\bar{3}14)$
50.064	50.064	50.064		(113)
		50.707	50.707	(025)
			53.173	(131)
			55.676	(413)
			56.349	$(\bar{2}25)$
			59.462	$(42\bar{1})$

Table S3: The exact position ($2\Theta\,/\,^\circ$) of the assigned diffractions of the PXRD patterns presented in Fig. S4b, and the corresponding Miller indices (hkl; obtained from Match! database). Materials I is calcite, material II composes calcite and vaterite as well, material III is amorphous, material IV is mostly nesquehonite ($MgCO_3.3H_2O$), material V is amorphous, while material VI is nesquehonite. Color coding used in the last column helps the assignment of the material.

$2\Theta/^\circ$ (I.)	$2\Theta/^\circ$ (II.)	calcite, vaterite (hkl)	$2\Theta/^\circ$ (IV.)	$2\Theta/^\circ$ (VI.)	vaterite, nesquehonite (hkl)
			13.558	13.558	$(10\bar{1})$
				18.061	(011)
	21.000	(002)	21.000		(002)
23.043	23.043	(102)	23.068	23.068	(200)
	24.934	(100)	24.782	24.782	$(\bar{1}03)$
	27.103	(101)	27.380	27.380	$(20\bar{2})$
29.386	29.386	(104)	29.405	29.405	$(21\bar{1})$
31.420		(006)	32.077	32.077	$(21\bar{2})$
	32.821	(012)	34.193	34.193	(021)
35.951	35.951	(110)	35.739	35.739	$(30\bar{1})$
39.389	39.389	(113)	41.582	41.582	$(30\bar{3})$
	40.769	(013)	44.380	44.380	(006)
43.136	43.136	(202)	45.337	45.337	(313)
	43.915	(110)	47.143	47.143	(223)
47.090		(204)	49.434	49.434	$(\bar{3}14)$
47.482	47.482	(108)	50.707	50.707	(025)
48.480		(116)	53.173	53.173	(131)
	49.160	(112)	55.676	55.676	(413)
	50.125	(014)	56.349	56.349	$(\bar{2}25)$
56.533		(211)	59.462	59.462	$(42\bar{1})$
	55.893	(202)			
57.368	57.368	(212)			

S5 Composition dependence of crystal sizes in case of various individual and composite systems

Table S4: Summary of crystal sizes in case of individual (top part) and composite (bottom part) alkaline earth metal–carbonate precipitate patterns (dense: where separated crystals were present; membranous: where the precipitate tube was observed; -: membrane structure was not present in the pattern; x: we could not prepare solution at this concentration). $c_{Na_2CO_3} = 1.5\,M$; $c_{MgCl_2} = 1.5\,M$; $Q = 1\,mL/min$; $V_{Na_2CO_3} = 5\,mL$.

c / M	Crystal size (μm)					
	Without magnesium					
	Ca(II)		Sr(II)		Ba(II)	
	dense	membranous	dense	membranous	dense	membranous
0.25	11.6±2.0	-	3.9±1.4	-	4.2±0.8	-
0.50	10.5±2.3	-	1.4± 0.2	-	2.5±0.4	-
0.75	7.1±0.8	-	0.9± 0.1	-	1.0±0.1	-
1.00	6.8±1.5	-	0.8±0.1	-	0.7±0.1	-
1.50	6.7±0.5	-	0.2±0.1	0.1±0.1	0.1±0.1	0.2±0.1
c / M)	**With magnesium**					
	Ca(II)		Sr(II)		Ba(II)	
	dense	membranous	dense	membranous	dense	membranous
0.25	0.4±0.1	-	0.5±0.1	-	0.1±0.1	-
0.50	0.8±0.1	7.0±0.1	3.9±0.3	6.3±0.1	0.9±0.2	-
0.75	3.1±0.1	5.0±0.3	4.6±0.1	6.0±0.1	x	x
1.00	5.0±0.4	5.5±0.8	4.7±0.3	5.1±1.2	x	x
1.50	6.2±0.2	0.1±0.1	x	x	x	x

S6 Composition dependence of crystal sizes in case of calcium containing pure and composite patterns

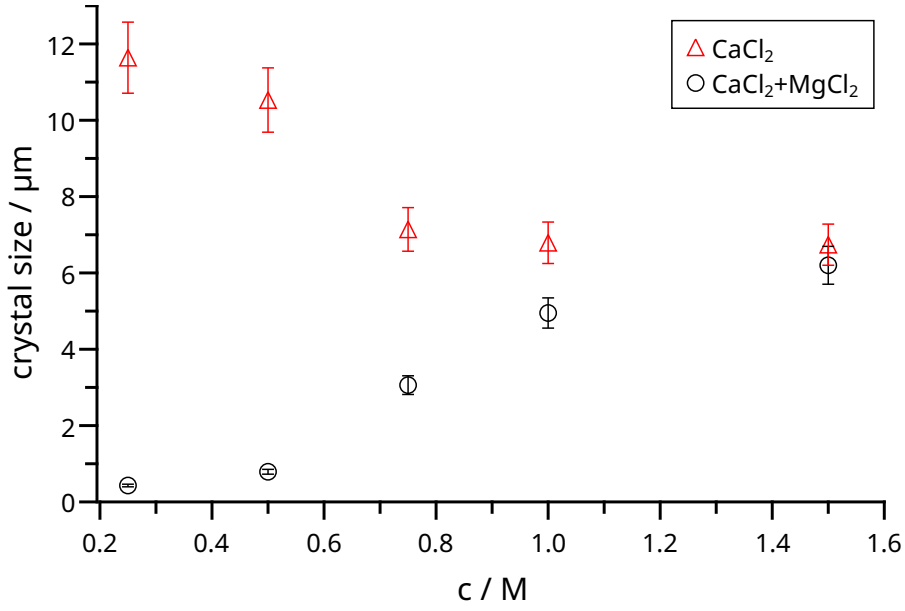

Figure S5: Calcium ion concentration dependence of the crystal size in case of calcium carbonate and calcium–magnesium–carbonate precipitate patterns. The samples were taken from the dense segment of the patterns. $c_{Na_2CO_3} = 1.5\,M$; $c_{MgCl_2} = 1.5\,M$; $Q = 1\,mL/min$; $V_{Na_2CO_3} = 5\,mL$.

S7 Stoichiometric ratio dependence of the crystal composition in case of various composite precipitates

Table S5: The composition of composite alkaline earth metal–carbonate precipitate patterns at different stoichiometric ratios (dense: where separated crystals were present; membranous: where the precipitate tube was observed; -: membrane structure was not present in the pattern; x: we could not prepare solution at this concentration; M(II): added Ca(II), Sr(II) and Ba(II)). $c_{Na_2CO_3} = 1.5\,M$; $c_{MgCl_2} = 1.5\,M$; $Q = 1\,mL/min$; $V_{Na_2CO_3} = 5\,mL$.

M(II) : Mg(II)	Ca(II) (at.%)				Sr(II) (at.%)			
	Ca(II)		Mg(II)		Sr(II)		Mg(II)	
	dense	membranous	dense	membranous	dense	membranous	dense	membranous
1.0 : 6.0	14.6±0.3	-	85.4±0.3	-	25.3±7.0	-	74.7±0.3	-
1.0 : 3.0	37.7±0.5	64.3±1.0	62.3±0.3	35.7±0.5	85.9±29.7	77.8±28.0	14.0±0.5	22.2±0.4
1.0 : 2.0	33.8±0.4	34.6±0.7	66.2±0.3	65.4±0.5	98.5±35.1	93.8±32.6	1.5±0.3	6.2±0.5
1.0 : 1.5	49.6±0.9	27.9±0.4	50.4±0.6	72.1±0.3	95.0±38.9	56.1±29.1	5.0±0.5	43.9±0.6
1.0 : 1.0	91.2±1.7	42.4±0.8	8.8±0.3	57.6±0.6	x	x	x	x

M(II) : Mg(II)	Ba(II) (at.%)			
	Ba(II)		Mg(II)	
	dense	membranous	dense	membranous
1.0 : 6.0	10.1±2.8	-	89.9±0.9	-
1.0 : 3.0	15.3±3.2	-	84.7±0.9	-
1.0 : 2.0	x	x	x	x
1.0 : 1.5	x	x	x	x
1.0 : 1.0	x	x	x	x

References

(1) L. Chen, J. Jiang, Z. Bao, J. Pan, W. Xu, L. Zhou, Z. Wu, and X. Chen, Synthesis of barium and strontium carbonate crystals with unusual morphologies using an organic additive, Russ. J. Phys. Chem. **2013**, *87*, 2239 – 2245.

(2) Q. Chen, T. Hui, H. Sun, T. Peng, and W. Ding, Synthesis of magnesium carbonate hydrate from natural talc, Open Chem. J. **2020**, *18*, 951 – 961.

(3) B. Boudaira, A. Harabi, F. Bouzerara, F. Zenikheri, L. Foughali, and A. Guechi, Preparation and characterization of membrane supports for microfiltration and ultrafiltration using kaolin (DD2) and $CaCO_3$, Desalination Water Treat. **2016**, *57*, 5258 – 5265.

(4) M.C. Reis, M.F.B. Sousa, F. Alobaid, C.A. Bertran, and Y. Wang, A two-fluid model for calcium carbonate precipitation in highly supersaturated solutions, Adv. Powder Technol. **2018**, *29*, 1571 – 1581.